FINE-SEDIMENT DEPOSITION FROM GRAVITY SURGES ON UNIFORM SLOPES

W. BRIAN DADE, JOHN R. LISTER, AND HERBERT E. HUPPERT
Institute of Theoretical Geophysics, Department of Earth Sciences and Department of Applied Mathematics and Theoretical Physics, University of Cambridge, Downing Street, Cambridge CB2 3EQ, UK

ABSTRACT: **The propagation of and the deposition from a noneroding, turbulent gravity surge are described by a simple model for a two-dimensional, well-mixed buoyant cloud of suspended particles moving down an inclined surface. The model includes the effects of entrainment of ambient seawater, deposition of suspended sediment, seafloor friction, and slope. Our results are applicable to large, decelerating turbidity currents and their distal deposits on uniform slopes in lakes and the sea. The scaling arguments that emerge from our analysis, moreover, have important ramifications for the design and interpretation of laboratory analogs of these phenomena.**

General solutions are obtained to the coupled equations that describe the evolution of momentum, total mass, and particulate mass of a surge. The solutions vary on two horizontal length scales: x_o, beyond which the behavior of the surge is independent of the initial momentum and shape; and x_r, beyond which the driving negative buoyancy of the surge is lost due to particle settling. For fine particles whose settling velocity is much less than the forward propagation speed of the surge, the suspension is well mixed and $x_o \ll x_r$. The deposit thickness diminishes as the inverse square root of the downstream distance x when $x_o \ll x \ll x_r$, and then diminishes exponentially with downstream distance as x approaches and exceeds x_r.

The length of a surge deposit scales with $x_r = kb_o\sin\theta/\gamma\rho_a(\overline{w}_s\cos\theta)^2$, where k is the assumed constant aspect ratio of the surge, b_o is the initial buoyancy per unit width at the point of issue onto a slope of constant angle θ, ρ_a is the ambient density, $\overline{w}_s$ is the average settling velocity of the suspended particles, and $\gamma = 6 + 8C_D/\alpha$ incorporates the ratio of the constant coefficients of drag C_D and fluid entrainment α.

Extension of our model to the case of two particle sizes indicates that, even for very poorly sorted suspensions, the estimate for the length of a surge deposit x_r is valid if $\overline{w}_s$ is defined as the volume-averaged settling velocity of the initial suspension at x_o. The ratio of coarse to fine material in model deposits generated from initially poorly sorted suspensions can diminish dramatically in the downstream direction, however, due to differential rates of gravitational settling.

INTRODUCTION

A gravity surge is a density-driven intrusion of a finite volume of one fluid into another fluid. Turbidity currents in lakes and the sea that result from the catastrophic and instantaneous failure of the seafloor are geologically important gravity surges driven by sediment dispersed throughout the intruding flow. The sediment and flow are intimately coupled because the particles are suspended within the current by turbulence generated by the flow and the flow is maintained by the negative buoyancy of the fine-particle suspension.

When a sediment-laden surge issues onto the shallow slopes of the continental rise and abyssal plain it ultimately dissipates due to the loss of excess density through entrainment of ambient seawater and deposition of suspended particles, and due to the damping of turbulence by boundary friction or internal density stratification. During passage across the shallow slopes of continental margins, however, a very large surge can generate a massive deposit that is 100–1000 km long and more than one meter thick (Pilkey et al. 1980). Commonly, however, surge deposits occur as beds of silt and fine sand each less than 20 cm thick (Nelson et al. 1978). The regional accumulation of fine sediment from successive turbidity currents issuing from the continental slope can result in a sediment fan that progrades into the deep-sea basin.

Turbidity currents and their deposits pose challenging problems for interpretation of marine sedimentary processes. Deep-sea turbidite deposits make up a significant fraction of the geologic record and play important roles in the formation of some petroleum reservoirs. Turbidites also document ongoing processes that can interfere with engineered offshore structures and that can lead to the downslope transport and ultimate deep-sea burial of pollutants present in shallow-water sediments.

Such considerations have motivated many workers to study small-scale suspension currents in the laboratory (Middleton 1966, 1967; Riddel 1972; Luthi 1980, 1981; Siegenthaler and Buhler 1985; Middleton and Neal 1989; Laval et al. 1988; Altinakar et al. 1990; Bonnecaze et al. 1993; Sparks et al. 1993). Turbidity currents in natural settings have also been studied (Normark 1987; Zeng et al. 1991), but in general are difficult to measure directly. Much of what geologists know of natural, deposit-forming surges is instead based on interpretation of the resulting deposits themselves (Johnson 1967; Komar 1970, 1985; Sadler 1982). The conceptual basis for these interpretations has been limited due to the unsteady and nonuniform nature of the flows responsible for the deposits.

Many of the existing models for gravity-current behavior devised for geological applications either (i) are based on the assumption of a steady balance between buoyancy and friction acting at the head or on a semi-infinite slab (e.g., Komar 1977) or (ii) have neglected the effects of sediment flux at the bed (Kirwan et al. 1986). Other studies that have analyzed the downstream evolution of a gravity surge (Chu et al. 1979; Fukushima et al. 1985; Siegenthaler and Buhler 1985; Parker et al. 1986; Eidsvik and Brørs 1989) have shown that the sediment flux at the sea floor, the frictional resistance and slope of the sea floor, and the turbulent entrainment of ambient seawater all control the changing state of the flow. These studies have not been able to predict the downstream evolution of the deposit characteristics, however, because to do so requires consideration of the behavior of an entire surge rather than merely the behavior at a point in an otherwise horizontally infinite flow.

The modified thermal model of Beghin et al. (1981) is the starting point for our analysis of sediment deposition from a turbidity surge. We have extended their analysis of a dense, well-mixed solute cloud propagating down a slope to accommodate the effects of friction and loss of driving, negative buoyancy through fine-particle settling. Our analysis is based on the assumptions that the particles are in well-mixed suspension and settle slowly relative to the speed of the flow. Friction and slope angle of the bed are assumed to be uniform. As a result, our model is readily applicable to the interpretation of large, channelized currents and their sand- and silt-rich deposits which occur in marine environments with a nonnegligible seafloor slope.

The inclusion of the effects of sediment deposition represents an advance from some earlier studies (e.g., Kirwan et al. 1986). We focus here only on the waning phase of a turbidity current from which sediments are indeed being deposited (in contrast to the model of Fukushima and Parker (1990), which was developed primarily to examine the effects of bed erosion on an accelerating snow avalanche). We reduce the governing equations for depositing surges to dimensionless forms and obtain predictions for the propagation and depositional behavior of surges. Our results shed light on trends in the surge-deposit thickness and grain size. In particular, we

JOURNAL OF SEDIMENTARY RESEARCH, VOL. A64, NO. 3, JULY, 1994, P. 423–432
 1073-130X/94/0A64-423/$03.00

show that the deposit varies in a predictable way over a characteristic run-out distance that is related to the downslope component of initial buoyancy and the average settling velocity of the particles suspended in the gravity surge. Applications to specific transport events will come with improved quantification of the model parameters that describe the physical processes governing the evolution of the surge.

In the following section we briefly review the conceptual basis for analyzing the behavior of gravity surges. We then present a mathematical statement of our model for deposit-forming gravity surges and explore the behavior of model surges, which we characterize first by a single settling velocity (as a dynamic measure of grain size) and then by two distinct settling velocities. In the final section, we discuss the implications of our model for the interpretation of natural surge deposits and of laboratory experiments designed as analogs of natural phenomena. A list of symbols is given at the end of the text.

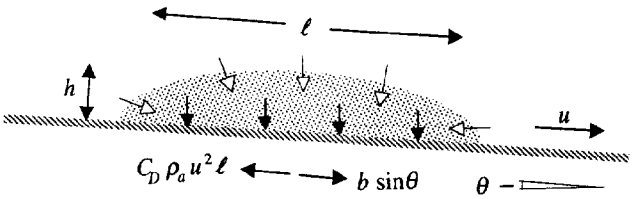

FIG. 1.—Schematic representation of a two-dimensional, deposit-forming gravity surge evolving as it propagates down a uniform slope. Conservation of total mass of the surge includes the effects of entrainment of ambient seawater; conservation of particulate mass includes the effects of sedimentation at the bed (arrows at boundaries of surge). Conservation of surge momentum reflects a balance between downslope component of buoyancy b and friction at the surge boundaries.

A BASIS FOR ANALYZING THE BEHAVIOR OF GRAVITY SURGES

Beghin et al. (1981) modified an existing theory for an unbounded, thermally driven plume (Morton et al. 1956), in order to describe the overall behavior of a dense, two-dimensional cloud of solute propagating down a sloping surface. The coupled equations describing changes in the momentum and mass of a buoyancy-conserving surge were used to show that the propagation speed u of such a cloud decreases in proportion to the inverse square root of the propagation distance x. Their result can be expressed as

$$\rho_a u^2 x = b_o f(\theta), \tag{1}$$

where ρ_a is the density of the ambient seawater, b_o is the constant buoyancy per unit width of the surge, and θ is the angle of the slope with the horizontal. The function $f(\theta)$ is related to a surge Froude number, which is of order unity and varies weakly with slope.

This relationship reflects a balance between the inertia, buoyancy, and entrainment of ambient fluid. As a result of this balance, the surge speed diminishes and the total momentum evolves with an associated increase in volume with downstream distance. In the derivation of the governing equations leading to Eq 1, Beghin et al. considered the surge shape and the coefficient describing the rate of entrainment of ambient fluid to be independent of downstream distance and functions of slope only. These assumptions are well supported by the results of laboratory experiments in which two-dimensional surges of saline water flow under fresh water down smooth slopes of between 1° and 90° (Beghin et al. 1981; Laval et al. 1988; Liu et al. 1991).

Kersey and Hsü (1976) provided theoretical arguments and supporting experimental observations which indicate that sustained surge propagation should occur in laboratory settings on slopes as low as 1/2°, and in natural settings on even less steep slopes due to a decrease in the drag coefficient with increasing flow Reynolds number. This notion is especially important in that most natural, deposit-forming surges occur on deep-sea fans and abyssal plains where θ is typically less than 1° (Nelson et al. 1978).

Even under shallow-slope conditions, sustained surge propagation is thus considered to result primarily from the drive of the downslope component of buoyancy and not from self-weight collapse. As in the study of Beghin et al. (1981) and motivated by the experimental observations, we consider that a turbidity surge can be modeled as a sediment-laden cloud of constant shape. This treatment reflects the fact that pressure gradients are eliminated in an analysis of the volume-averaged behavior of a surge. As a result, they do not influence the sustained propagation of the center of gravity of the surge. One implication of this perspective is that no sustained travel can occur on perfectly horizontal surfaces; some nominal slope is required to provide the driving buoyancy.

The analysis by Beghin et al. and the experimental confirmation of their predictions provide an extremely useful starting point for our consideration of a slowly depositing gravity surge. Such a surge initially adjusts to the state described by Eq 1 and then evolves due to the slow loss of buoyancy through fine-particle settling. We now turn our attention to the development of a model that describes this evolution.

A MODEL FOR DEPOSITING GRAVITY SURGES

Basic Equations for Suspensions of a Single Particle Size

Following the analysis of Beghin et al. (1981), we consider the behavior of a well-mixed, two-dimensional, sediment-laden cloud on a surface of uniform slope and roughness (Fig. 1). We propose that this particular configuration is applicable, for example, to a large surge that is confined to a fjord, a channel in a deep-sea fan, or a narrow abyssal plain with a regional slope. The propagation of the surge reflects a balance between the downslope drive, friction, entrainment of ambient seawater, and the slow depositional loss of buoyancy.

These elements of the surge dynamics can be described quantitatively in terms of the two-dimensional cloud volume $q = h\ell$, where h is the volume-averaged height and ℓ is the total length of the surge, the volume-averaged velocity u, and the buoyancy $b = g\Delta\rho q$ of the suspension with excess density $\Delta\rho$. Each of these properties of the surge is important in its evolution. The equations describing this evolution are those governing the variation of the total linear momentum of the surge

$$\frac{d\rho_a(1 + C_A)qu}{dt} = b \sin\theta - C_D\rho_a u^2\ell \tag{2a}$$

[rate of change of momentum = downslope component of buoyancy force − frictional drag force along surge length],

the increase in the total mass of the surge

$$\frac{dq}{dt} = \alpha u\ell \tag{2b}$$

[rate of change of volume = rate of net entrainment of ambient fluid along surge length],

and the loss of particulate mass from a surge that is well-mixed, relatively dilute, and non-eroding (e.g., Martin and Nokes 1988; Bonnecaze et al. 1993)

$$\frac{db}{dt} = -\frac{\overline{w_s} b \cos\theta}{h} \tag{2c}$$

[rate of change of buoyancy = loss of particulate mass due to settling at the bed along surge length].

In Eq 2a, C_A and C_D are coefficients describing the volume-averaged effects of added mass and friction (in excess of that required to maintain the surge shape). The added-mass coefficient represents the momentum associated with the motion in the ambient fluid caused by passage of the

underlying surge. It can be approximated by that of an elliptical cylinder, for which $C_A = 2h/\ell$ (Batchelor 1983). For the elongate shapes considered here C_A is negligible.

The coefficient α in Eq 2b relates the rate of entrainment of ambient seawater to the downstream rate of propagation of the surge and is assumed to be a function of the slope angle θ only (Turner 1986). Entrainment occurs both at the head and along the length of the surge at the interface between the suspension and the ambient fluid, and for the elongate surges considered here we scale entrainment with the surge length ℓ. To do otherwise would simply require the introduction of a shape factor with a value of order unity.

In Eq 2c, $\overline{w_s}$ represents the characteristic settling velocity of individual particles in the suspension. The downward flux of suspended particles is expressed as in Eq 2c because particles arrive at the bed primarily by gravitational settling through a near-bed viscous sublayer (Dade et al. 1991). In the case of very fine sand and silt, $\overline{w_s}$ is proportional to the square of the average particle diameter. Because we are concentrating here on surges carrying fine sediment in well-mixed, turbulent suspension, we assume for all cases that $\overline{w_s}/u \ll 1$. Because we are interested in deposit-forming phenomena, however, a key assumption of our analysis is that there is net deposition of fine sediment from the surge. Any reentrainment of newly settled material reduces the net downward flux of a suspension and causes the current to deposit over a greater distance. The increased propagation distance could be modeled empirically by selection of a suitably reduced average velocity of particle settling.

Eqs 2a–c are solved subject to the initial conditions u_o, q_o, and b_o that reflect the state of the surge at the point x_o where it first exhibits invariant shape on a seafloor of constant slope and uniform bed roughness. The true origin of the surge is upstream of this point.

Eqs 2a and 2b constitute the basic model considered by Beghin et al. (1981) and lead to the result given in Eq 1, although we have extended Eq 2a to include the effects of friction. Eq 2c is introduced here to include the effects of particle settling.

Dimensional Analysis

The height and length of a surge can be expressed in terms of the surge volume q and the constant aspect ratio

$$k = h/\ell \tag{3a}$$

by

$$h = (kq)^{1/2} \tag{3b}$$

and

$$\ell = (q/k)^{1/2}. \tag{3c}$$

Substituting Eq 3c into Eq 2b and transforming the time derivative to a spatial derivative by using $u = dx/dt$, we find upon integration of the result that the surge volume per unit width q is given by

$$q = \frac{\alpha^2}{4k}x^2 \tag{4a}$$

where the origin of the downslope coordinate x has been defined such that

$$x_o = \frac{2}{\alpha}(kq_o)^{1/2} \tag{4b}$$

In buoyancy-conserving flows $\overline{w_s} \equiv 0$ and $b \equiv b_o$. Under these conditions, insertion of Eq 4a into Eq 2a, transformation of the time derivative to a spatial derivative and integration of the result yields

$$u^2 = u_c^2\left(\frac{x_o}{x}\right) + (u_o^2 - u_c^2)\left(\frac{x_o}{x}\right)^{4(1+C_D/\alpha)} \tag{5a}$$

where u_c is a characteristic velocity scale defined by

$$u_c^2 = \frac{8k^{1/2}\sin\theta}{\gamma\alpha}\frac{b_o}{\rho_a q_o^{1/2}} \tag{5b}$$

and

$$\gamma = 6 + \frac{8C_D}{\alpha}. \tag{5c}$$

In the far field where $x \gg x_o$, Eq 5a reduces to

$$\rho_a u^2 x = b_o\left(\frac{16k\sin\theta}{\gamma\alpha^2}\right) = b_o f_2(\theta, C_D) \tag{6a}$$

where $f_2(\theta, 0) = f(\theta)$, in agreement with the expression found by Beghin et al. (1981) and given in Eq 1 of the previous section. In terms of the characteristic length and velocity scales x_o and u_c, Eq 6a can be written as

$$U \equiv \frac{u}{u_c} = \left(\frac{x_o}{x}\right)^{1/2} \tag{6b}$$

which indicates that in the far field the propagation speed of a buoyancy-conserving surge is inversely proportional to the square root of the propagation distance x.

Eqs 3–6 constitute the analytical results of Beghin et al. (1981) for buoyancy-conserving surges, extended here to include the effects of friction in the parameter γ. If drag is neglected this parameter takes the value of 6, and the importance of the initial condition decays like $(x/x_o)^{-4}$. With the inclusion of friction, $\gamma > 6$ and the rate of decay of the initial condition is even greater. In natural settings where surges enter a region of interest in "running order", that is, where $u_o \approx u_c$, the far-field behavior is achieved almost immediately. In general the initial momentum of a surge thus quickly becomes irrelevant, and the behavior of the surge is well-described by Eq 6 at downstream distances beyond the entry length x_o.

These results provide the basis for analyzing the effects of a relatively slowly depositing suspension. If $\overline{w_s}$ is constant and small (just how small will be made clear in Eq 10b), then the suspension can be assumed to be well-mixed, and the far-field behavior of surge propagation speed represented in Eq 6 can be achieved before significant loss of buoyancy through deposition has occurred. Under these conditions, we can use Eq 2c to identify the length scale x_r over which slow deposition of the suspended particles takes place. As outlined in the appendix, this length scale is given by

$$x_r = \frac{k\,b_o\sin\theta}{\gamma\rho_a(\overline{w_s}\cos\theta)^2}. \tag{7}$$

This depositional run-out distance is thus proportional to the aspect ratio of the surge, the initial buoyancy, and the slope angle, and is inversely proportional to the combined effects of fluid entrainment and friction and to the square of the particle settling velocity. It reflects a kinematic balance between the rates of buoyancy loss, volume increase, and momentum decay as a surge evolves downstream.

We now introduce several dimensionless variables. The two dependent variables, which are motivated by the form of Eq 6a and by the magnitude of the initial buoyancy, are

$$\psi^2 = \left(\frac{u}{u_c}\right)^2\frac{x}{x_o} \tag{8a}$$

and

$$B = b/b_o \tag{8b}$$

both of which are unity for buoyancy-conserving flows. Recalling from Eqs 3 and 4 that the thickness of a fluid-entraining surge is proportional to the propagation distance, we see that ψ^2 can be interpreted as a di-

mensionless measure of the mean kinetic energy per unit length of the flow. We also note that

$$\psi^2/B \equiv \left(\frac{u^2 q^{1/2}}{b}\right) \Big/ \left(\frac{u_c^2 q_o^{1/2}}{b_o}\right) = Fr^2/Fr_o^2 \tag{9a}$$

so that the ratio of the variables ψ^2 and B is a measure of the Froude number $Fr = u/(gh\Delta\rho/\rho_a)^{1/2}$ of a surge relative to the value Fr_o when it has achieved a buoyancy-driven state. In terms of the function $f_2(\theta, C_D)$ introduced in Eq 6a, the initial Froude number is given by

$$Fr_o^2 = \frac{\alpha}{2k} f_2(\theta, C_D) \tag{9b}$$

or, equivalently,

$$Fr_o^2 = \frac{\sin\theta}{C_D + 3\alpha/4}. \tag{9c}$$

The relationship given in Eq 9c is analogous to the findings of earlier studies that considered horizontally uniform, buoyancy-conserving gravity currents (e.g., Komar 1977).

We also introduce the independent variable

$$\xi^2 \equiv x/x_r \tag{10a}$$

which measures the downstream distance relative to the distance required for significant loss of buoyancy through slow deposition of the suspended particles.

If a slowly depositing surge is to achieve conditions leading to the behavior described by Eq 6, x_o must be much less than x_r, or equivalently

$$\xi_o^2 \equiv \frac{x_o}{x_r} = \left(\frac{4\overline{w}_s \cos\theta}{\alpha u_c}\right)^2 \ll 1. \tag{10b}$$

Eq 10b reflects the condition that the particle concentration in a surge initially decreases through entrainment of ambient fluid rather than through deposition. If this condition is not met, then there is strong interaction between fluid entrainment and sediment deposition in the near field. Consequently, the far-field behavior does not approach that of a buoyancy-conserving surge, and the surge propagation and deposit geometry reflect the initial conditions. If the condition of Eq 10b is satisfied, on the other hand, then the suspension is well mixed and the far-field behavior of a buoyancy-conserving surge is readily attained.

In terms of the new variables ψ, B, and ξ, Eqs 2a and 2c can be transformed from temporal to spatial coordinates and then, as is shown in the appendix, reduced to

$$\frac{d\psi^2}{d\xi} = \gamma \frac{B - \psi^2}{\xi} \tag{11a}$$

and

$$\frac{dB}{d\xi} = -\frac{B}{\psi} \tag{11b}$$

with upstream boundary conditions

$$\psi^2 = B = 1 \text{ at } \xi = \xi_o \ll 1. \tag{11c}$$

Eqs 2a–c seem to be the simplest possible model that retains the essential physics of a deposit-forming gravity surge on a uniform slope. We have reduced these equations to Eq 4a and the pair of coupled, nonlinear, ordinary differential equations of Eq 11 in terms of the dimensionless variables ψ, B, and ξ defined in Eqs 8 and 10. Whereas the original governing equations incorporate many parameters, the reduced equations depend only on the single coefficient γ defined in Eq 5c. Thus a wide variety of suspension-driven surges can be described by solutions that are dependent on only one parameter.

Normalized Propagation Speed and Deposit Thickness

Before discussing the solutions to Eq 11, we introduce descriptions of additional properties of a deposit-forming surge in suitably normalized terms. The relative speed of downslope propagation is

$$U \equiv u/u_c = (\xi_o/\xi)\psi \tag{12}$$

where $U = 1$ at $\xi = \xi_o \ll 1$.

The areal density of a deposit (mass per unit area) at a point along the travel path can be evaluated from the loss of particulate mass during the finite time of transit of the surge over that point. Because the overall time scale of deposition is long compared with this transit time, the local deposition rate is approximated by that occurring when the center of gravity of the surge passes over the point of interest. Calculated in this way, the deposit density is given by

$$\delta = -\frac{\rho_s}{g(\rho_s - \rho_a)} \frac{db}{dx} \tag{13a}$$

where δ is the mass per unit area of the bed, which is proportional to the uncompacted thickness of the deposit, and ρ_s is the density of individual particles. Substitution of the initial values into Eq 13a yields an estimate for the initial deposit density δ_o,

$$\delta_o = \frac{\rho_s}{g(\rho_s - \rho_a)} \frac{\overline{w}_s \cos\theta}{u_c} \frac{b_o}{(kq_o)^{1/2}}. \tag{13b}$$

The deposit density (or thickness) relative to that observed near the effective origin of the surge is then

$$\eta \equiv \delta/\delta_0 = -(\xi_0/\xi)\, dB/d\xi \tag{13c}$$

so that $\eta = 1$ at $\xi = \xi_o \ll 1$. Referring to Eq 11b, we see that

$$\eta = \frac{\xi_o}{\xi} \frac{B}{\psi}. \tag{13d}$$

With the substitution of Eqs 9a and 12 into Eq 13d and rearrangement of the result, we obtain the potentially useful relationship

$$\frac{\eta}{U} = \frac{Fr_o^2}{Fr^2}. \tag{14}$$

The left side of Eq 14 corresponds to a similarity variable introduced by Siegenthaler and Buhler (1985, 1986) as the "thickness number" T'. We will consider this result in more detail in the discussion.

Model Results for Suspensions of a Single Particle Size

The results of our model predict the far-field conditions associated with the generation of fine-grained, distal deposits by turbidity surges of catastrophic origin in lakes or the deep sea. The nondimensionalization used in Eqs 8–12 allows us to consider the general behavior of these phenomena in terms of the single parameter γ defined in Eq 5c.

Using a fourth-order Runge-Kutta scheme, we obtained numerical solutions for $\gamma = 46$ (corresponding to $C_D/\alpha = 5$) and $\gamma = 6$ ($C_D = 0$). The results of our integrations are presented in Figure 2, which shows the dimensionless kinetic energy ψ^2, buoyancy B, propagation speed U, Froude number Fr, and density η of the resulting deposit, each as a function of $\xi^2 = x/x_r$, for a suspension-driven gravity surge characterized by a single particle-settling velocity. There is little difference between the curves for the two representative end-member values of γ, as will be discussed in more detail below.

A useful representation of a surge once the initial conditions have been forgotten can be determined analytically from power-series solutions to Eq 11. We find that

$$\psi = 1 - \frac{\gamma}{2(\gamma + 1)}\xi + O(\xi^2) \quad \text{and} \quad B = 1 - \xi + O(\xi^2) \tag{15a}$$

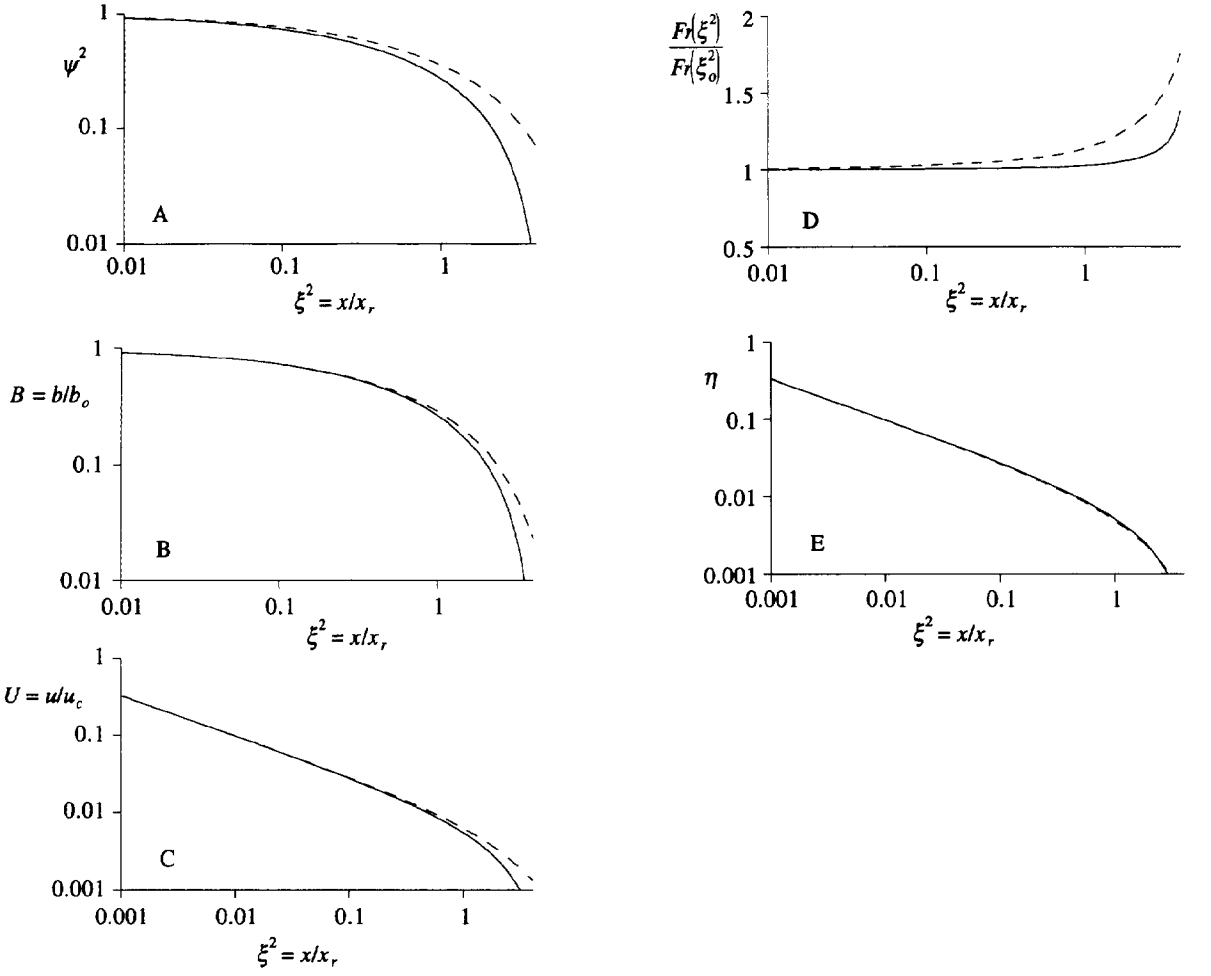

FIG. 2.—Calculations of the downslope evolution of a suspension-driven surge and its resulting deposit as functions of the dimensionless downstream distance $\xi^2 = x/x_r$. The calculations are for the simplest case of a suspension characterized by a single settling velocity and $\xi_o^2 = 10^{-4}$. The solid lines in each panel correspond to the case $C_D/\alpha = 5$; the dashed lines correspond to the friction-free case $C_D = 0$. **A)** Dimensionless kinetic energy per unit length of the flow. **B)** Relative buoyancy. **C)** Relative speed of downslope propagation. **D)** Relative Froude number. **E)** Relative thickness of deposit.

where $O(\xi^2)$ represents a small correction of order ξ^2. Inserting these relationships into Eqs 12 and 13c indicates that

$$U = \frac{\xi_o}{\xi}[1 + O(\xi)] \quad \text{and} \quad \eta = \frac{\xi_o}{\xi}[1 + O(\xi)]. \tag{15b}$$

Eq 15 (as well as Eq 16 introduced below) provides a check on our numerical calculations and yields relationships that may be compared directly with field observations. For example, it follows from Eq 15b that if $\xi^2 \ll 1$, corresponding to $x_o \ll x \ll x_r$, then both the propagation speed and the deposit thickness are proportional to the inverse square root of the downstream distance x. In fact $U \approx \eta$. As we showed earlier, the quantity $\psi B^{-1/2}$ corresponds to the surge Froude number which, from Eq 15a, remains relatively constant. Mathematically, this is a consequence of the fact that γ is sufficiently greater than 1 to ensure that the product $\psi B^{-1/2}$ departs little from unity when $x_o \ll x \ll x_r$. Thus the exact value of γ is relatively unimportant in that reach. The physical interpretation is that the Froude number of a surge driven by a fine-particle suspension is relatively well conserved as a consequence of the very slow evolution of the surge due to depositional loss of buoyancy.

The numerical solutions also indicate that a deposit-forming gravity surge decays to a relatively buoyancy-free state over a propagation distance corresponding to $\xi^2 \approx 1$ (Fig. 2A–C). Up to this run-out distance, as discussed above, the relative kinetic energy and buoyancy of the flow are virtually identical functions of the propagation distance. The normalized mean propagation speed and density of deposit are also virtually identical functions of the propagation distance. At values of ξ^2 approaching and exceeding unity, however, the buoyancy of the surge diminishes more rapidly than its speed, and the Froude number increases dramatically due to the inertia of the surge. The distance at which $\xi^2 \approx 1$ also corresponds to a "pinch-out" length beyond which the relative deposit density (or thickness) essentially vanishes (Fig. 2E).

The behavior of the surge in this regime can be described analytically by using the numerically determined result that $B \ll \psi^2$ when $\xi^2 \gg 1$. With this approximation it is straightforward to show from Eq 11 that

$$\psi \sim C_1 \xi^{-\gamma/2} \quad \text{and} \quad B \sim C_2 \exp\left[-\frac{2}{C_1(2+\gamma)}\xi^{\gamma/2+1}\right] \tag{16a}$$

where C_1 and C_2 depend only on γ and are obtained from the solutions for $\xi^2 \ll 1$. From Eq 16a we see that ψ^2 decays algebraically (slowly) and B decays exponentially (rapidly), in agreement with the numerical pre-

diction that $B \ll \psi^2$ for $\xi^2 \gg 1$. Using these approximations for the relative speed U and deposit density η, we find that

$$U \sim C_1 \xi_o \xi^{-\gamma/2-1} \quad \text{and} \qquad \eta \sim (\xi_o C_2/C_1)\xi^{\gamma/2-1}\exp\left[-\frac{2}{C_1(2+\gamma)}\xi^{\gamma/2+1}\right]. \tag{16b}$$

Eq 16b indicates that, as a suspension-driven surge approaches and surpasses x_r, the propagation speed decays algebraically and the thickness of the resulting deposit decreases exponentially with further distance in the downstream direction. Beyond x_r the driving buoyancy is lost through deposition, and the surge is essentially a bounded, suspension-free jet with residual momentum that is lost rapidly through friction and entrainment of ambient fluid. Accordingly, the precise rate of decay of a surge in this region is strongly dependent on the magnitude of the bed friction relative to fluid entrainment as embodied in the parameter γ. The overall Froude number, as calculated in relative terms by the quantity $\psi B^{-1/2}$, increases dramatically in this regime due to the inertia of the dilute surge.

Suspensions of Two Grain Sizes

Geologists are often interested in the sorting pattern of at least two nominal size classes (sand and silt, say), so it is useful to consider the end-member case of a suspension with two distinct modal settling velocities. Under these conditions, an equation describing the conservation of mass in each grain-size class is needed, so that Eq 2c is expanded to

$$\frac{db_c}{dt} = -\frac{w_c b_c \cos\theta}{h} \quad \text{and} \quad \frac{db_f}{dt} = -\frac{w_f b_f \cos\theta}{h} \tag{17}$$

for the coarse and fine fractions, denoted respectively by the subscripts c and f. We now introduce additional dimensionless variables to describe the case of a bimodal suspension. We make the contribution of each size class to the total buoyancy relative to the initial total value b_o by defining

$$B_c = b_c/b_o \quad \text{and} \quad B_f = b_f/b_o \tag{18a}$$

so that

$$B_{co} + B_{fo} = 1. \tag{18b}$$

We now define a characteristic settling velocity $\overline{w_s}$ to be the average of the settling velocities of the two size classes weighted by their initial proportions B_{co} and B_{fo}, so that

$$\overline{w_s} = w_c B_{co} + w_f B_{fo} \tag{19a}$$

Accordingly, the settling velocity of each size class is normalized with respect to the weighted average

$$W_c = w_c/\overline{w_s} \text{ and } W_f = w_f/\overline{w_s}. \tag{19b}$$

If Eqs 17 are made dimensionless using Eqs. 8a, 10a, 18a and 19b, we obtain the following two new expressions which describe the conservation of buoyancy in each size class

$$\frac{dB_c}{d\xi} = -W_c\frac{B_c}{\psi} \quad \text{and} \quad \frac{dB_f}{d\xi} = -W_f\frac{B_f}{\psi} \tag{20}$$

This scheme preserves the essential scaling behavior of Eqs 8–11 where the length scale x_r is defined in terms of the average settling velocity $\overline{w_s}$ of the initial suspension. The requirement that $x_o \ll x_r$ still applies. The relative deposit density η_i of grain-size class i is calculated from $dB_i/d\xi$ using equations analogous to Eq 13c.

Model Results for Suspensions of Two Grain Sizes

We obtained numerical solutions to Eqs 11a and 20 for the case of equal concentrations of coarse and fine material for which the settling velocity of the coarse sediments is ten times that of the fine material. The calculated values of the dimensionless kinetic energy ψ^2, propagation speed U, buoyancy B, Froude number Fr, and density η of the resulting deposit are shown in Figure 3. Our calculations for the bimodal case indicate that the presence of relatively fine sediments in the surge results in a somewhat greater run-out distance than that of a surge driven by a well-sorted suspension with an equivalent average settling velocity (Fig. 3A–D). This effect is due to the protracted life of a suspension with a fine-grained component.

Importantly, however, the downstream trends in the normalized thickness of model deposits outlined above are relatively insensitive to the distribution of particle sizes in the initial suspension, even for this rather contrived bimodal case (Fig. 3E). At a downstream distance corresponding to $\xi^2 \approx 1$ the deposit thickness still shows the onset of an exponential decrease with further distance in the downstream direction. We conclude that the concept of a deposit pinch-out at x_r remains useful. Moreover, our calculations show that the ratio of coarse to fine sediment in a model deposit from a poorly sorted suspension can evolve significantly in the downstream direction due to differential rates of settling of the respective size classes in suspension.

DISCUSSION

We have reported here a straightforward model that describes the downstream evolution of a turbidity surge and its distal deposit. The model incorporates the essential governing processes of entrainment of ambient seawater and fine-particle settling as well as the dynamic balance between the downslope drive due to buoyancy and the opposing drag due to fluid entrainment and bottom friction.

Defining the fluid entrainment rate as a fraction of the average surge speed implies invariance in turbulent structure at the fluid interface of a surge during the evolution of the surge. Alternative approaches include relating the entrainment velocity either to the Reynolds stress at the interface or to the overall Richardson number of the flow. For example, relating α to an overall Richardson number would incorporate some effects of stratification. However, the Richardson number is inversely proportional to the Froude number, which we have shown remains relatively constant during much of the evolution of the surge. Turner (1986) reviewed many successful applications of the entrainment assumption to natural phenomena representing a wide range of scales, and concluded that the present approach, wherein α is taken to be a constant, is indeed a useful one. It is important to note that the value of the coefficient α reflects the net effects of entrainment of ambient fluid and detrainment of the suspension in vortices shed from the current (see fig. 2 of Laval et al. 1988). In the different situation of a flow on a horizontal surface α may even be negative (Hallworth et al. 1993).

Modifications that could make our model more realistic, but that would detract from its straightforward investigation, include the addition of terms describing sediment reentrainment at the bed and three-dimensional spreading of a debouching surge beyond the point of issue from a source canyon. Neither of these processes is well understood at present, but it is evident that sediment reentrainment leads to a greater deposition length, whereas three-dimensional spreading reduces the deposition length. If the interstitial fluid of a surge is less dense than the ambient, as may occur if lighter surface waters were carried to depth by the surge, then loss of the excess bulk density of the surge through deposition ultimately leads to positive buoyancy of the flow. As a result, the surge lifts off from the seafloor (Sparks et al. 1993) and the deposit may be truncated. Additional calculations (not shown here) that include Coriolis acceleration of the surge predict progressive deflection of the travel path and may contribute to an understanding of the transformation of waning gravity currents into contour currents. A further possibility is the addition to Eqs 2a–c of a fourth equation that describes the evolution of turbulent kinetic energy. This

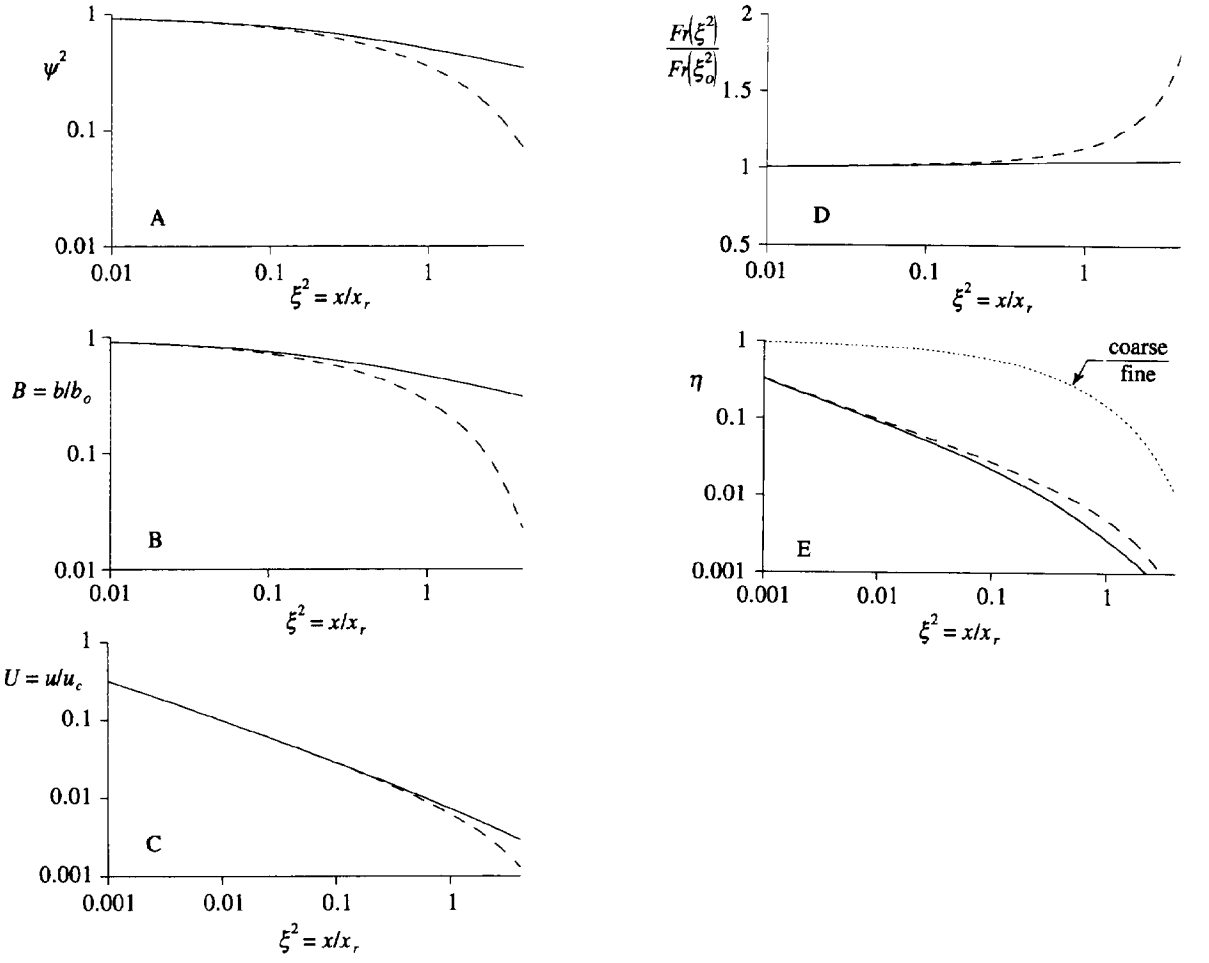

FIG. 3.—Calculations of the downslope evolution of a suspension-driven surge and its resulting deposit as functions of the dimensionless downstream distance ξ^2. The calculations are for $\xi_o^2 = 10^{-4}$. The solid lines in each panel correspond to the behavior of a frictionless surge with a bimodal distribution of grain sizes in suspension. The ratio of settling velocities of the fine and coarse size classes is 1:10, and the initial mass of the fine particles is equal to that of the coarse particles. The dashed lines correspond to the frictionless single-grain-size case plotted in Figure 2 and shown again here for comparison. **A)** Dimensionless kinetic energy per unit length of the flow. **B)** Relative buoyancy. **C)** Relative speed of downslope propagation. **D)** Relative Froude number. **E)** Relative thickness of deposit. The dotted line in **E** represents the ratio of coarse to fine material in the deposit relative to the value of this ratio near the origin.

modification may be necessary to accommodate the effects of density stratification and turbulence suppression in the suspension (Fukushima and Parker 1990). Stratification may be especially important in the rapid emplacement of thick, homogeneous muds from very densely concentrated flows (McCave and Jones 1988). We plan to explore some of these phenomena.

We propose, however, that relationships for geological interpretation of distal, fine-grained turbidites laid down in fjords or channels in deep-sea fans can be obtained from the present, straightforward analysis. We envisage three stages of downstream evolution in the thickness of these deposits (Fig. 4). The earliest stage of behavior of a deposit-forming surge is dominated by its initial state and the characteristics of the deposit will reflect these conditions (region A in Fig. 4). Thus we suggest that, while a surge that has newly issued from a canyon adjusts to shallow-slope conditions the rapidly decelerating flow generates a deposit of relatively uniform thickness. The deposit thickness may even increase in the downstream direction if the initial speed is sufficient to cause sediment reentrainment at the bed. On the other hand, while a surge accelerates from an initial state of rest, as in most laboratory experiments, the deposit thickness near the point of release reflects the history of this flow acceleration.

At distances approaching and beyond the entry length x_o, the deposit thickness ultimately diminishes with downstream distance as the initial conditions of the surge are overcome and suspended material is progressively lost through slow settling. In this second stage the decrease in deposit thickness proceeds as the inverse square root of distance in the downstream direction (region B). This trend reflects flow conditions in which the surge propagation speed is also proportional to the inverse square root of downstream distance but in which the overall Froude number of the surge is relatively constant. In this reach the propagation speed and deposit thickness of a surge are closely related, as are the mean kinetic energy and buoyancy of the surge.

At downstream distances approaching and beyond the relaxation distance x_r the buoyancy and deposit thickness of a surge decrease exponentially with further travel downstream (region C). These "pinch-out" deposits thus correspond to flow conditions in which the driving buoyancy has been spent and the surge has degenerated into a relatively particle-free, bounded jet that dissipates rapidly due to friction and due to the

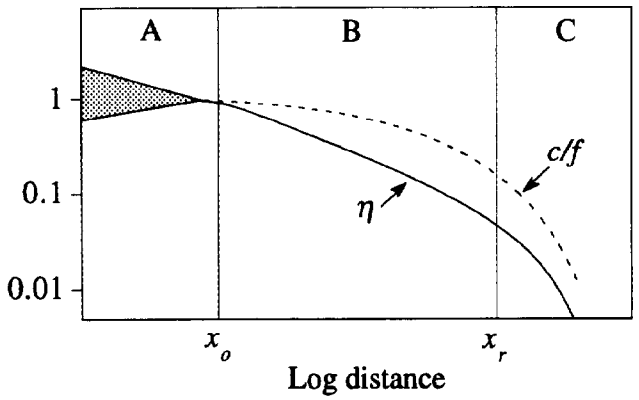

FIG. 4.—Schematic interpretation of trends in thickness and grain-size sorting in distal turbidites generated by noneroding gravity surges on uniform slopes. The horizontal axis represents the logarithm of distance x from the origin of a surge. The solid line shows model trends in the deposit thickness (h) relative to the thickness near the origin. The dashed line shows model trends in the ratio of coarse to fine material (c/f) in deposits relative to the value assumed by this ratio near the origin. The shaded area in region A indicates a possible range of deposit thickness that reflects dependence on the initial properties of the surge. See discussion in text for further details.

TABLE 1.—*Scaling quantities of representative, suspension-driven surges**

Quartz-Density Particles in Water:	ρ_o = 1000 kg m^{-3} A natural surge	ρ_s = 2600 kg m^{-3} A laboratory analog
θ	0.2°	1.0°
α	0.0092	0.033
k	0.1	0.2
C_D	0.004	0.005
q_o	0.1 km^2	400 cm^2
b_o	1.6 × 10^8 kg s^{-2}	12.5 kg s^{-2}
$\overline{w_s}$	0.43 cm s^{-1}	0.028 cm s^{-1}
Stokes diameter	70 μm	18 μm
u_c	7.1 m s^{-1}	13 cm s^{-1}
x_o	22 km	5.4 m
x_r	318 km	77 m
δ_o	156 kg m^{-2}	5.1 mg cm^{-2}
$\overline{w_s}\cos\theta/\alpha u_c$	0.065	0.065
$f_2^{1/2}(\theta, C_D)$	2.65	2.65
Fr_o	0.57	0.76
Re_o	7.1 × 10^8	1.1 × 10^4

* $Fr_o = (\rho_a u_c^2 \ell_o / b_o)^{1/2}$ is an overall Froude number and $Re_o = u_c h_o/\nu$ is the initial flow Reynolds number for a dilute surge in terms of the initial surge length $\ell_o = (q_o/k)^{1/2}$, initial thickness $h_o = (kq_o)^{1/2}$ and kinematic viscosity ν of the ambient fluid.

entrainment of ambient fluid. The grain size of the deposits generated from poorly sorted suspensions decreases downstream. In such deposits there is thus a strong relationship between deposit thickness and grain size. The actual form of this relationship reflects the distribution of grain size in the initial suspension.

The prospect that the surge propagation speed and the thickness of a resulting deposit are mutually related in the main body of a surge deposit offers an important scaling relationship of potential use to geologists. Recall from Eq 14 that $\eta/U = Fr_o^2/Fr^2$. Using the definitions of the parameters developed earlier in our analysis, this result can be reexpressed in terms of quantities that are measurable in the field as

$$g_b'\delta_t/\overline{w_s} = u\cos\theta/(k\,Fr^2) \tag{21}$$

where δ_t is the actual bed thickness observed locally and $g_b' = g\phi_b(\rho_s - \rho_a)/\rho_a$ is the "bed buoyancy" in terms of the volumetric fraction of solids ϕ_b in the bed. The terms on the left side of Eq 21 represent quantities that can be estimated from a surge deposit, and we note in particular that the product $g_b'\delta_t$ is independent of the effects of bed consolidation. The ratio of these quantities may be used to infer the combination of hydraulic conditions of the gravity surge that gave rise to the deposit—surge propagation speed u, slope θ, aspect ratio k, and overall Froude number $Fr = u/(gh\Delta\rho/\rho_a)^{1/2}$.

For a Froude number close to unity and a given settling velocity of particles in a suspension on a known slope, either a more voluminous or a more densely concentrated cloud results in a thicker deposit. These properties of the deposit-forming cloud also contribute, however, to the speed with which the cloud propagates across the seafloor. Thus δ_t and u are related as reflected by Eq 21. A longer and thinner surge, moreover, results in greater and more prolonged local rates of sediment deposition. Thus the deposit thickness is inversely proportional to the surge aspect ratio k.

The scaling given in Eq 21 is a modified form of the "thickness number" defined by Siegenthaler and Buhler (1985) as

$$T' = g_b'\delta_t/u^2 \tag{22}$$

in their analysis of the equations governing the evolution of a suspension-driven surge. Basing their arguments on dimensional reasoning for self-similar flows, Siegenthaler and Buhler proposed that T' is constant and independent of the size of the sediments in suspension. Their measurements of deposits from laboratory surges driven by suspensions characterized by a range of particle settling velocities tentatively supported this conclusion. We hasten to point out, however, that in these experiments neither the ratio $\overline{w_s}/u$ nor the ratio x_o/x_r was sufficiently small for proper development of the self-similar behavior in surges described by our model. When Siegenthaler and Buhler (1986) applied their scaling to the geologic record, moreover, they curiously redefined T' with a denominator corresponding to the square of the settling velocity of the largest particle in a local deposit rather than to u^2 and found that the resulting ratio increased by several orders of magnitude along the length of a deposit. From our analysis we find that a more informative scaling of the quantity defined in Eq 22 is weighted by the ratio $u/\overline{w_s}$. Our analysis also yields the explicit dependence of T' on the aspect ratio and overall Froude number of a surge, both of which reflect hydraulic conditions that are dependent on the slope angle θ. These improvements are included in the scaling given in Eq 21.

APPLICATIONS

We illustrate the application of our predictions to both natural surges and laboratory experiments with calculations based on representative values (Table 1) for aqueous flows. In these examples, ambient depth and stratification are assumed not to influence the behavior of the flow.

The data of Laval et al. (1988) indicate that the dimensionless grouping $k/(\gamma\alpha^2)$ is a function of the slope angle θ given by

$$k/(\gamma\alpha^2) \approx 25\theta^{-1} \tag{23}$$

for $0 < \theta < 10°$. This relationship implies that the function $f_2(\theta, C_D)$ is relatively independent of θ for small slopes. It also implies that because the surge aspect ratio k is finite, the fluid entrainment coefficient α vanishes as θ tends to zero. We use Eq 23 to evaluate α for specified values of the aspect ratio of a surge and characteristics of the bed.

Consider, for example, a surge with an initial height of 100 m, an initial length of 1 km, a volumetric sediment concentration of order 10^{-1} and an effective suspension settling velocity corresponding to 70 μm-diameter particles with the density of quartz. Such a cloud would travel with an initial speed $u_c \approx 7$ m/s within $x_o \approx 20$ km or so of its point of entry onto a uniform, deep-sea slope of 0.2°. Any potential for reentrainment of newly deposited sediment due to the initially large propagation speed reinforces our view that buoyancy is relatively well conserved in this upper reach and that the suspension-driven surge achieves far-field behavior. In

the far field, the surge would propagate approximately three hundred kilometers while depositing the bulk of its driving suspension and would rapidly dissipate thereafter. Calculations using Eq 4 indicate that the surge would have grown in thickness from 100 m to over 1 km and in length from 1 km to over 10 km due to the entrainment of seawater during the time required to traverse this "run-out" distance.

The thickness of the resulting deposit would be about 10 cm (based on $\delta_o \approx 150$ kg/m^2 and a volumetric density of the bed of 0.5) near the point of issue of the surge (or point of earliest deposition in the case of significant reentrainment), and would diminish with the inverse square root of distance in the reach $x_o \ll x \ll x_r$, or 20 km $\ll x \ll$ 320 km. The deposit would rapidly "pinch out", however, at distances approaching and exceeding 320 km. A significant mixture of coarse and fine fractions, such that the average settling velocity of the initial suspension still corresponds to that of 70 μm particles, would extend the life of the surge considerably but would not substantially alter the estimate for the length of the deposit. In this case, however, a dramatic decrease in the ratio of coarse to fine material would be observed in the deposit at downstream distances approaching 320 km. The conditions described here may well correspond to those that deposited many turbidites of silt and fine sand in sloping channels in deep-sea fans (e.g., Nelson et al. 1978).

Consider, on the other hand, a laboratory surge with an initial volume per unit width of 400 cm^2 and a solids concentration of 0.02 that is released from rest onto a smooth floor with a slope of 1°. Such a flow would approximate the propagation and deposition behavior of the natural phenomenon described above if it comprised a suspension of quartz-density particles with an average diameter of 18 μm. This equivalence is based on equal values of the ratio $\overline{w}_s\cos\theta/\alpha u_c$ of the settling velocity to the fluid-entrainment velocity, which implies (from Eq 10b) equal values of the ratio x_o/x_r of the acceleration length scale to the deposition length scale. That such similitude is required of laboratory experiments was recognized in early studies (Middleton 1966), but here we point out three important aspects of this scaling that emerge from our analysis. Firstly, if $\overline{w}_s\cos\theta/\alpha u_c$ is sufficiently small then analogous behavior is achieved during the far-field history of the laboratory surge regardless of the exact value. Thus experiments to model the far-field behavior should use particles of diameter no greater than 18 μm. Secondly, owing to the difficulty of replicating the initial conditions, analogous behavior may not be achieved for several meters (corresponding approximately to the near-field entry length x_o) downstream from the point of release of the surge even if the values of $w_s\cos\theta/\alpha u_c$ are identical. Thirdly, if the value of $\overline{w}_s\cos\theta/\alpha u_c$ for a laboratory surge is insufficiently small, then much of the suspended material settles out during the earliest stages of flow while the surge is accelerating from rest, and the far-field behavior is not realized. During the period in which the flow is dominated by the initial conditions, such a surge and its deposits may be better described by models for suspension-driven, lock-release gravity currents that undergo self-weight collapse from an initial position of rest (Bonnecaze et al. 1993; Dade and Huppert 1994).

CONCLUSIONS

An analysis of the equations that govern the behavior of noneroding, suspension-driven gravity surges on slopes yields scaling relationships for the propagation of surges and the geometry of the resulting deposits. These relationships provide a new basis for the quantitative interpretation of fine-grained turbidites comprising many deep-sea sediments. Important tasks that we are now addressing include tests of the scaling relationships through laboratory experimentation and examination of the geologic record. Although our approach is developed with special reference to fine-grained turbidity currents on gentle slopes, our results may also apply under certain conditions to distal deposits generated during the waning stages of other suspension-driven gravity surges, including subaerial fine-grained ash flows and powder-snow avalanches.

ACKNOWLEDGMENTS

We thank R.T. Bonnecaze, R.E. Britter, M. Hampton, I.N. McCave, G.V. Middleton, H. Pantin, G. Parker, and J.S. Turner for helpful comments on earlier versions of the text. This research has been supported by the Natural Environmental Research Council (WBD and HEH) and The Royal Society (JRL).

REFERENCES

Altinakar, S., Graf, W.H., and Hopfinger, E.J., 1990, Weakly depositing turbidity current on a small slope: Journal of Hydraulic Research, v. 28, p. 55–80.

Batchelor, G.K., 1983, An Introduction to Fluid Dynamics: Cambridge University Press, 615 p.

Beghin, P., Hopfinger, E.J., and Britter, R.E., 1981, Gravitational convection from instantaneous sources on inclined boundaries: Journal of Fluid Mechanics, v. 107, p. 407–422.

Bonnecaze, R.T., Huppert, H.E., and Lister, J.R., 1993, Particle-driven gravity currents: Journal of Fluid Mechanics, v. 250, p. 339–369.

Chu, F.H., Pilkey, W.D., and Pilkey, O.H., 1979, An analytical study of turbidity current steady flow: Marine Geology, v. 33, p. 205–220.

Dade, W.B., and Huppert, H.E., 1994, A box model for non-entraining, suspension-driven gravity surges on horizontal surfaces: Sedimentology, in press.

Dade, W.B., Nowell, A.R.M., and Jumars, P.A., 1991, Mass arrival mechanisms and clay deposition at the seafloor, *in* Bennett, R.H., Bryant, W.R., and Hulbert, M.H., eds., Clay Microstructure: From Muds to Shale: New York, Springer-Verlag, p. 161–166.

Eidsvik, K.J., and Brørs, B., 1989, Self-accelerated turbidity current prediction based upon (k-ϵ) turbulence: Continental Shelf Research, v. 9, p. 617–627.

Fukushima, Y., and Parker, G., 1990, Numerical simulation of powder-snow avalanches: Journal of Glaciology, v. 36, p. 229–237.

Fukushima, Y., Parker, G., and Pantin, H.M., 1985, Prediction of ignitive turbidity currents in Scripps Submarine Canyon: Marine Geology, v. 67, p. 55–81.

Hallworth, M.A., Phillips, J.C., Huppert, H.E., and Sparks, R.S.J., 1993, Entrainment in turbulent gravity currents: Nature, v. 362, p. 829–831.

Johnson, M.A., 1967, Application of theory to an Atlantic turbidity current path: Sedimentology, v. 7, p. 117–129.

Kersey, D.G., and Hsü, K.J., 1976, Energy relations of density current flows: an experimental investigation: Sedimentology, v. 23, p. 761–789.

Kirwan, A.D., Doyle, L.J., Bowles, W.D., and Brooks, G.R., 1986, Time-dependent hydrodynamic models of turbidity currents analyzed with data from the Grand Banks and Orleansville events: Journal of Sedimentary Petrology, v. 56, p. 379–386.

Komar, P.D., 1970, The competence of turbidity current flow: Geological Society of America Bulletin, v. 81, p. 1555–1562.

Komar, P.D., 1977, Computer simulation of turbidity current flow and the study of deep-sea channels and fan sedimentation, *in* Goldberg, E.D., McCave, I.N., O'Brien, J.J., and Steele, J.H., eds., The Sea, Vol. 6: New York, Wiley, p. 603–621.

Komar, P.D., 1985, The hydraulic interpretation of turbidites from their grain sizes and sedimentary structures: Sedimentology, v. 32, p. 395–407.

Laval, A., Cremer, M., Beghin, P., and Ravenne, C., 1988, Density surges: two-dimensional experiments: Sedimentology, v. 35, p. 73–84.

Liu, Q., Shläpfer, D., and Bühler, H., 1991, Motion of dense thermals on incline: Journal of Hydraulic Engineering, v. 117, p. 1588–1599.

Luthi, S., 1980, Some new aspects of two dimensional turbidity currents: Sedimentology, v. 28, p. 97–105.

Luthi, S., 1981, Experiments on non-channelized turbidity currents and their deposits: Marine Geology, v. 40, p. M59–M68.

Martin, D., and Nokes, R., 1988, Crystal settling in a vigorously convecting magma: Nature, v. 332, p. 534–536.

McCave, I.N., and Jones, K.P.N., 1988, Deposition of ungraded muds from high-density non-turbulent turbidity currents: Nature, v. 333, p. 250–252.

Middleton, G.V., 1966, Small scale models of turbidity currents and the criterion for autosuspension: Journal of Sedimentary Petrology, v. 36, p. 202–208.

Middleton, G.V., 1967, Experiments on density and turbidity currents. 3: Deposition of sediment: Canadian Journal of Earth Sciences, v. 4, p. 475–505.

Middleton, G.V., and Neal, W.J., 1989, Experiments on the thickness of beds deposited by turbidity currents: Journal of Sedimentary Petrology, v. 59, p. 297–307.

Morton, B.R., Taylor, G.I., and Turner, J.S., 1956, Turbulent gravitational convection from maintained and instantaneous sources: Royal Society (London), Proceedings, v. A234, p. 1–23.

Nelson, C.H., Normark, W.R., Bouma, A.R., and Carlson, P. R., 1978, Thin-bedded turbidites in modern submarine canyons and fans, *in* Stanley, D.J., and Kelling, G., eds., Sedimentation in Submarine Canyons, Fans, and Trenches: Stroudsburg, Pennsylvania, Dowden, Hutchinson & Ross, p. X–X.

Normark, W.R., 1987, Observed parameters for turbidity-current flow in channels, Reserve Fan, Lake Superior: Journal of Sedimentary Petrology, v. 59, p. 423–431.

Parker, G., Fukushima, Y., and Pantin, J.M., 1986, Self-accelerating turbidity currents: Journal Fluid Mechanics, v. 171, p. 145–181.

Pilkey, O.H., Locker, S.D., and Cleary, W.J., 1980, Comparison of sand-layer geometry on flat floors of 10 modern depositional basins: American Association of Petroleum Geologists Bulletin, v. 64, p. 841–856.

Riddel, J.F., 1972, A laboratory study of suspension-effect density currents: Canadian Journal of Earth Sciences, v. 6, p. 231–246.

Sadler, P.M., 1982, Bed-thickness and grain size of turbidites: Sedimentology, v. 29, p. 37–51.

SIEGENTHALER, C., AND BUHLER, J., 1985, The kinematics of turbulent suspension currents (turbidity currents) on inclined surfaces: Marine Geology, v. 64, p. 19–40.

SIEGENTHALER, C., AND BUHLER, J., 1986, The reconstruction of the paleo-slope of turbidity currents, based on simple hydromechanical parameters of the deposit: Acta Mechanica, v. 63, p. 235–244.

SPARKS, R.S.J., BONNECAZE, R.T., HUPPERT, H.E., LISTER, J.R., HALLWORTH, M.A., MADER, H., AND PHILLIPS, J., 1993, Sediment-laden gravity currents with reversing buoyancy: Earth and Planetary Science Letters, v. 114, p. 243–257.

TURNER, J.S., 1986, Turbulent entrainment: the development of the entrainment assumption, and its application to geophysical flows: Journal of Fluid Mechanics, v. 173, p. 431–471.

ZENG, J., LOWE, D.R., PRIOR, D.B., WISEMAN, W.J., AND BORNHOLD, B.D., 1991, Flow properties of turbidity currents in Bute Inlet, British Columbia: Sedimentology, v. 38, p. 975–996.

Received 26 July 1993; accepted 18 November 1993.

APPENDIX

Nondimensionalization of the Governing Equations for a Suspension-Driven Surge

In this appendix we describe one approach to the analysis that leads to the scaling of the equations and the explicit non-dimensional forms of Eqs 11a and 11b.

Eqs 2 are rewritten in terms of the variables $q(x)$, $u(x)$, and $b(x)$ by using Eq 3 and $d/dt = u\,d/dx$ to obtain

$$\frac{dq}{dx} = \alpha(q/k)^{1/2} \tag{A1a}$$

$$u\frac{d(qu)}{dx} = \frac{b\sin\theta}{\rho_a} - C_D u^2(q/k)^{1/2} \tag{A1b}$$

and

$$u\frac{db}{dx} = -\frac{\overline{w}_s b\cos\theta}{(kq)^{1/2}}. \tag{A1c}$$

Before proceeding with a detailed manipulation of these equations we can obtain powerful results by simple estimates of the magnitude of the terms in Eq A1. If b is slowly varying then from Eqs A1a and A1b

$$q/x \sim \alpha(q/k)^{1/2} \tag{A2a}$$

and

$$u^2[q/x + C_D(q/k)^{1/2}] \sim b_o\sin\theta/\rho_a \tag{A2b}$$

where $\sim$ denotes an order-of-magnitude balance. The scales of x_o and u_c in Eqs 4b and 5b can then be obtained from Eq A2 upon using $q \sim q_o$. We can also see from Eq A2 that q is proportional to x^2 and that u^2 is proportional to $x^{-1/2}$, in agreement with Eqs 4a and 6.

The slowly varying buoyancy b varies over the length scale x_r given from Eq A1c by

$$u/x_r \sim \overline{w}_s\cos\theta/(kq)^{1/2} \tag{A3}$$

By substituting $q \sim q_o(x_r/x_o)^2$, $u \sim u_c(x_o/x_r)^{1/2}$ and the estimates of x_o and u_c into Eq A3, we obtain

$$x_r \sim x_o\left(\frac{\alpha u_c}{\overline{w}_s\cos\theta}\right)^2 \sim \frac{kb_o\sin\theta}{\rho_a(\overline{w}_s\cos\theta)^2} \tag{A4}$$

in agreement with Eqs 7 and 10b. The nondimensionalization of Eq 11 is motivated by these scalings.

We proceed with the derivation as follows. Eq [A1a] can be integrated analytically to obtain Eq 4. After the elimination of q, Eq A1b can be put in the form

$$x^2\frac{du^2}{dx} + \frac{1}{2}(\gamma + 2)xu^2 = \frac{8kb_o\sin\theta}{\rho_a\alpha^2}B. \tag{A5}$$

Writing the differentials of the dimensionless variables defined in Eqs 8 and 10 in the forms

$$d\psi^2 = (x\,du^2 + u^2dx)/x_o u_c^2 \tag{A6a}$$

and

$$x\frac{d}{dx} = \frac{1}{2}\xi\frac{d}{d\xi} \tag{A6b}$$

we can reduce Eq A2 to

$$\frac{1}{2}\xi\frac{d\psi^2}{d\xi} + \frac{1}{2}\gamma\psi^2 = \left(\frac{8kb_o\sin\theta}{\rho_a\alpha^2}\frac{1}{x_o u_c^2}\right)B. \tag{A7}$$

With further rearrangement and use of the definitions for x_o and u_c given in Eqs 4b and 5b, Eq 11a is readily obtained.

Similarly, q is eliminated from Eq A1c and the transformation Eq A6b used to obtain

$$\frac{\xi}{2}\frac{dB}{d\xi} = -\frac{2\overline{w}_s\cos\theta}{\alpha u}B. \tag{A8}$$

Recalling from Eq 12 that $\psi = (\xi u/\xi_o u_c)$, we see that Eq A8 can be written as

$$\frac{dB}{d\xi} = -\frac{4\overline{w}_s}{\alpha u_c\xi_o}\frac{B}{\psi}. \tag{A9}$$

With the definition of x_r given in Eq 7 (and hence ξ_o by Eq 10b), Eq A9 reduces to Eq 11b.

*Symbols**

$b \equiv g\Delta\rho q$; buoyancy $[MT^{-2}]$
$b_o \equiv$ buoyancy at x_o $[MT^{-2}]$
$b_c \equiv$ buoyancy of coarse fraction $[MT^{-2}]$
$b_f \equiv$ buoyancy of fine fraction $[MT^{-2}]$
$B \equiv b/b_o$
$C_A \equiv$ coefficient of added mass
$C_D \equiv$ coefficient of friction
$Fr \equiv u/(gh\Delta\rho/\rho_a)^{1/2}$; Froude number
$Fr_o \equiv$ Froude number at x_o
$h \equiv$ surge height $[L]$
$g \equiv$ acceleration due to gravity $[LT^{-2}]$
$g_b' \equiv g\phi_b(\rho_s - \rho_a)/\rho_a$; bed buoyancy $[LT^{-2}]$
$k \equiv h/\ell$; surge aspect ratio
$\ell \equiv$ surge length $[L]$
$q \equiv$ surge volume per unit width $[L^2]$
$q_o \equiv$ surge volume at x_o $[L^2]$
$t \equiv$ time $[T]$
$T \equiv g_b'\delta_o/u^2$; thickness number
$u \equiv$ surge speed $[LT^{-1}]$
$u_o \equiv$ surge speed at x_o $[LT^{-1}]$
$u_c \equiv$ characteristic speed of surge $[LT^{-1}]$
$U \equiv u/u_c$
$w_c \equiv$ settling velocity of coarse fraction $[LT^{-1}]$
$w_f \equiv$ settling velocity of fine fraction $[LT^{-1}]$
$\overline{w}_s \equiv$ average settling velocity $[LT^{-1}]$
$W_c \equiv w_c/\overline{w}_s$ and $W_f \equiv w_f/\overline{w}_s$
$x \equiv$ downstream distance $[L]$
$x_o \equiv$ entry length $[L]$
$x_r \equiv$ run-out length $[L]$
$\alpha \equiv$ coefficient of fluid entrainment
$\delta \equiv$ deposit mass per unit area of seafloor $[ML^{-2}]$
$\delta_o \equiv$ deposit density at x_o $[ML^{-2}]$
$\delta_t \equiv$ deposit thickness $[L]$
$\gamma \equiv 6 + C_D/\alpha$
$\eta \equiv \delta/\delta_o$
$\psi^2 \equiv u^2x/u_c^2x_o$
$\phi \equiv$ volume fraction of solids in suspension
$\phi_b \equiv$ volume fraction of solids in the bed
$\rho_a \equiv$ density of the ambient fluid $[ML^{-3}]$
$\Delta\rho \equiv \phi(\rho_s - \rho_a)$; excess density of the surge $[ML^{-3}]$
$\rho_s \equiv$ density of sediment particles $[ML^{-3}]$
$\theta \equiv$ angle of the seafloor with the horizontal
$\xi^2 \equiv x/x_r$
$\xi_o^2 \equiv x_o/x_r$

* Mass $[M]$, length $[L]$ and time $[T]$.